

2D-3D Face Recognition via Restricted Boltzmann Machines

Xiaolong Wang¹, Vincent Ly¹, Rui Guo² and Chandra Kambhamettu¹

¹University of Delaware, Newark, DE, U.S.A.

²The University of Tennessee, Knoxville, U.S.A.

Keywords: Restricted Boltzmann Machines, Canonical Correlation Analysis, Heterogeneous Face Recognition, Matching, Feature Extraction.

Abstract: This paper proposes a new scheme for the 2D-3D face recognition problem. Our proposed framework mainly consists of Restricted Boltzmann Machines (RBMs) and a correlation learning model. In the framework, a single-layer network based on RBMs is adopted to extract latent features over two different modalities. Furthermore, the latent hidden layer features of different models are projected to formulate a shared space based on correlation learning. Then several different correlation learning schemes are evaluated against the proposed scheme. We evaluate the advocated approach on a popular face dataset-FRGCV2.0. Experimental results demonstrate that the latent features extracted using RBMs are effective in improving the performance of correlation mapping for 2D-3D face recognition.

1 INTRODUCTION

Over the past few years, face recognition remains one of the most popular topics in machine learning and computer vision. Application based on face recognition technology (FRT) has been widely used in many areas such as security and multimedia. However, the recognition performance still degrades when affected by factors, such as illumination, pose and expression. To alleviate these influences, some researchers try to conduct face recognition via other modalities, such as Near-infrared (NIR) and 3D. 3D data, especially, has been widely used in face recognition. Recently, facilitated by the emerging low cost 3D sensing devices, such as Microsoft Kinect, Asus Xtion PRO, a large variety of RGB-Depth sensing techniques have been deployed to biometric signal aggregation and processing (Shotton et al., 2011). Meanwhile, 2D-3D heterogeneous face recognition has also attracted more interests. Heterogeneous face recognition refers to matching face images across different modalities.

Compared with face recognition using visible images, heterogeneous face recognition is more challenging, as illustrated in Figure.1. The individual's identity from 2D image is difficult to be determined using a 3D depth image. The difficulty is due to the dissimilar appearances of the 2D face image and the 3D face image. In this work, we focus on face recognition from 2D to 3D.

Compared to visible face recognition, the works

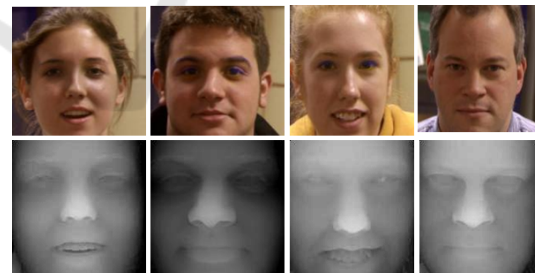


Figure 1: Examples of 2D and 3D face images. 2D faces (first row) associated with their corresponding depth image(second row).

related with heterogeneous face recognition between 2D and 3D are not widely studied. In (Rama et al., 2006), Partial Principal Component Analysis (P^2CA) was used to extract features and reduce features dimension in the 3D and 2D data separately. Their experimental results revealed that P^2CA could minimize the influence of illumination. Riccio et al.(Riccio and Dugelay, 2005) proposed to use predefined control points to calculate the geometrical invariants to correct the pose variation for 2D/3D face recognition. Afterwards, many researchers discovered the effectiveness of Canonical correlation learning (CCA) in this problem. Yang et al. (Yang et al., 2008) adopted CCA to learn the mapping relation among corresponding patches between 2D texture image and 3D depth image. The idea of utilizing CCA as the major technique for mapping between two different

modalities is also applied in work (Huang et al., 2012; Wang et al., 2013).

The aim of correlation learning is to maximize the intra-class similarity of the same individual within the projected subspace. As we know, CCA is a standard algorithm for calculating the linear projection of two random vectors which are maximally correlated. Kernel canonical correlation analysis (KCCA) extends CCA into nonlinear projection. KCCA performs better at capturing the maximally correlated nonlinear projection. It tries to find kernel Hilbert spaces with kernel functions. CCA and KCCA are adopted in learning features of multiple modalities, then can be used in fusion for classification (Sargin et al., 2007); especially under the situation when two modalities are used in the training phase and only one modality is available in the prediction phase. There are lots of applications across many different areas, such as natural language analysis (Vinokourov et al., 2002; Dhillon et al., 2011), age estimation (Guo and Wang, 2012), signal processing across multimodals (Slaney and Covell, 2000). The success of aforementioned works sheds the light in the research of heterogeneous 2D/3D face mapping which highlights the significance of correlation learning.

Recently, RBM is found to be effective in learning correlation among multi-modalities (Ngiam et al., 2011; Srivastava and Salakhutdinov, 2012). As a member of the Boltzmann Machine family, RBM attracts a resurgent study interest by inheriting the excellent ability of representation learning in an iterative way. Through the weights and offset parameters adjusting, the bipartite structured net efficiently learns the nested abstractions from the raw data from high dimension space. RBM benefits itself in terms of the hierarchical feature extraction ability and the unsupervised training manner. Facilitated by these merits, RBM is found to be effective. As we know, for cross modality learning, data from two different modalities is only available during the training phase. During the testing phase, only the data from a single modality is available. Therefore, learning an efficient single modality feature has become one essential step in this matching work. In (Ngiam et al., 2011), Ngiam et al. demonstrated that an auxiliary non-linear network can capture the relationship among different modalities. Motivated by their work, we plan to explore the feasibility of feature learning using single-layer network in 2D/3D face recognition.

There are several novelties in our work. First, a single-layer network is introduced to deal with the face recognition problem between 2D and 3D coupled with correlation mapping. Based on our knowledge, this is the first time that RBM model has been

adopted in heterogeneous face recognition. The proposed method offers better performance relative to the existing correlation learning schemes. This scheme can also be adopted in other related heterogeneous recognition works. The experimental results demonstrate the effectiveness of our scheme compared with reliance only on the correlation learning scheme. Second, to measure the generality of this scheme, different correlation methods have been compared for efficiency along with the layer features (2D RBM and 3D RBM features). In addition, the matching performance between two different modalities of different facial parts has been analyzed.

The rest of the paper is structured as follows. In Section 2, we introduce the proposed scheme. Experimental results are discussed in Section 3, and Section 4 provides conclusions.

2 OUR APPROACH

In this section, we describe our approach for the task of 2D-3D face recognition. Figure 2 shows an overview of our scheme. After pre-processing and extracting the feature from the images, RBM is conducted. Then correlation learning is performed to learn the projection matrix within each region between the two modalities. This will help project features of different modalities into a shared representation space. In general, our scheme mainly includes four parts, which are raw feature extraction (including image pre-processing), latent feature extraction (using RBM), correlation learning and matching. In the following paragraph, we will introduce the main algorithms used in each part.

2.1 Restricted Boltzmann Machines

Recently, deep learning has been widely used in machine learning and computer vision. One of the famous works is trying to examine how deep sigmoidal networks can help obtain better representation for handwritten classification (Hinton and Salakhutdinov, 2006). The key part is to conduct multi-layer training based on Restricted Boltzmann Machines (RBMs). This scheme achieved excellent classification results on this sort of problems.

RBM belongs to the category of Markov Random Field. Compared with Boltzmann Machines (BMs), RBMs further restrict BMs to the connection between visible-visible layer and hidden-hidden connections (within the intra-layers). An RBM bipartite structure can be illustrated as in Figure 3, where w is the weight connecting the hidden layers (h) and visible layers (v).

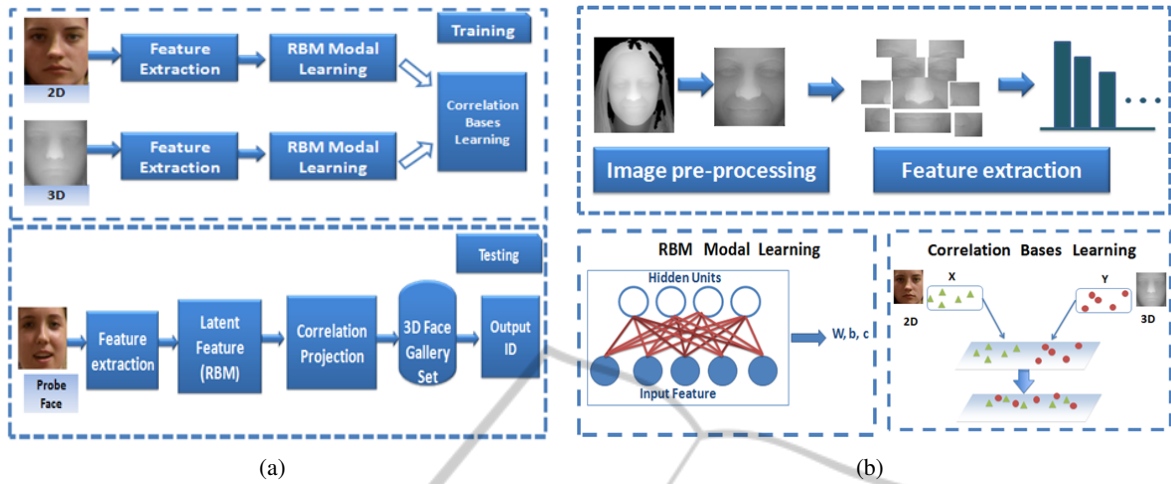


Figure 2: The proposed framework for 2D-3D face recognition.(a) Illustration of training and testing scheme. During the training phase, corresponding 2D and 3D face images of the same individual are used to learn RBM model and correlation basis. During the testing phase, we firstly extract 2D probe image feature. Then after hidden latent feature extraction and correlation projection, the probe images will be matched against the gallery set to get the corresponding ID. (b) Illustration of principal components of the proposed scheme. For the Pre-processing section, all the images (2D/3D) are cropped to the same size. The pre-processing of 3D images also include image denoising and hole filling. In our work, face is first divided into eleven facial parts, then feature extraction and RBM model learning is conducted within each part. The output latent 2D and 3D features acquired from RBM model are used to learn the basis of correlation learning model.

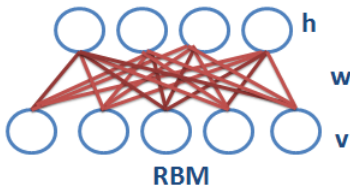


Figure 3: Illustration of RBM structure, where h indicates the hidden unit and v indicates visible unit. w is the weight connecting v and h .

From the model illustrated in Figure 3, we find that RBM is not a direct graphical model comprised of hidden variables(h) and visible variables(v). In addition, there is no connection between the variables of the same layer (e.g. within visible or hidden layer). The energy function $E(v,h)$ of an RBM is formulated as:

$$E(v,h) = -\sum_i b_i v_i - \sum_j c_j h_j - \sum_{i,j} W_{ij} v_i h_j \quad (1)$$

where W_{ij} represents the weight between the visible layer unit i and hidden layer unit j . The parameters c and b indicate the basis of hidden and visible layers respectively. The parameters W_{ij} , c and b can be estimated using maximum likelihood parameter estimation (Hinton and Salakhutdinov, 2006). This scheme can help minimize the energy states drawn from the data distribution and raise the energy states which are improbable given the data (Bengio, 2009). The joint

probability distribution is calculated as

$$P(v,h) = \frac{\exp(-E(v,h))}{Z} \quad (2)$$

where $Z = \sum_{v,h} \exp(-E(v,h))$ indicates the Boltzmann partition function. We can also calculate the marginal distribution of the visible units by summing up the possible hidden units, which can be calculated as

$$P(v) = \frac{1}{Z} \sum_h \exp(-E(v,h)) \quad (3)$$

With regard to the RBM structure listed in Figure 3, the units in visible and hidden layers are conditionally independent. When the units are binary, which means $v, h \in [0, 1]$, the probabilistic version of the neuron activation can be represented as:

$$\begin{aligned} P(v_i = 1|h) &= \text{sigm}(b_j + W_j^i h) \\ P(h_j = 1|v) &= \text{sigm}(c_i + W_i^j v) \end{aligned} \quad (4)$$

Compared with the binary input values, real valued data can be well modeled using Gaussian RBM (GRBM) (Hinton and Salakhutdinov, 2006). GRBM does a good job at modeling continuous multivariate data. There are many applications using GRBM, including action recognition (Wang et al., 2011), speech recognition (Mohamed et al., 2012), etc. In general, GRBM can be regarded as a mixture of diagonal Gaussians with shared W , c and b param-

eters. Its energy function is defined as follows:

$$E'(v, h) = -\frac{1}{2} \sum_i \frac{(v_i - b_i)^2}{\sigma_i^2} - \sum_{i,j} W_{ij} v_i h_j - \sum_j c_j h_j \quad (5)$$

Under this model, the conditional distributions for inference and generation are calculated as follows:

$$P(v_i | h) = N(b_i + \sigma_i^2 \sum_j W_{ij} h_j, \sigma_i^2) \quad (6)$$

$$P(h_j = 1 | v) = \text{sigm}(c_j + \sum_i W_{ij} v_i)$$

where $N(\cdot)$ denotes the Gaussian density, and sigm is the logistic function. In our work, GRBM is applied to learn the single data representation.

2.2 CCA

Canonical correlation analysis(CCA) (Sutton and Barto, 1998) has been widely used in multivariate analysis. It was first advocated by Hotelling (Hotelling, 1936) to calculate the basis vectors for two related multidimensional variables and can be used to maximize the correlation between these two sets of related variables. CCA methods have been widely used in machine learning and computer vision problems, such as action recognition(Kim et al., 2007), face recognition(Li et al., 2009). After projecting the data to high-dimensional space, CCA can be modeled as the relation between these two sets of variables. Suppose (x, y) is the corresponding data set. It includes N pairs of samples x_i, y_i . CCA is used to learn the projection matrix w_x and w_y to maximize the correlation between the projected matrix $w_x^T x$ and $w_y^T y$. That is to maximize the following correlation equation:

$$v = \frac{w_x^T C_{xy} w_y}{\sqrt{w_x^T C_{xx} w_x w_y^T C_{yy} w_y}} \quad (7)$$

where C_{xx} and C_{yy} indicate the intra-class covariance matrices. v is the correlation coefficient. And C_{xy} and C_{yx} indicate the inter-class covariance matrices. Because v is invariant to the scaling of w_x and w_y , CCA optimization problem can be equivalent to maximizing $w_x^T C_{xy} w_y$. This subjects to $w_x^T C_{xx} w_x = 1$ and $w_y^T C_{yy} w_y = 1$. (Hardoon et al., 2004) shows w_x can be solved by using the following eigenvalue problem,

$$C_{xy} C_{yy}^{-1} C_{yx} w_x = \lambda^2 C_{xx} w_x \quad (8)$$

where λ is the eigenvalue associated with the eigenvector w_x . To stabilize the solution, regularization

terms r_x and r_y are always added to each data set (Hardoon et al., 2004). Then v becomes

$$v = \frac{w_x^T C_{xy} w_y}{\sqrt{w_x^T (C_{xx} + \lambda I) w_x w_y^T (C_{yy} + \lambda I) w_y}} \quad (9)$$

Experiment results prove that Regularized CCA(rCCA) performs better than CCA in our work.

2.3 Kernel CCA

Because of its linearity, CCA may not be a good solver when dealing with some nonlinear correlation problems (Hardoon et al., 2004). Kernel CCA (KCCA) performs better than CCA in finding nonlinear projection of the two views (Hardoon et al., 2004). The main idea of KCCA is to project the data into a higher-dimension feature space using kernel functions. In this paper, we use the Gaussian kernel as the kernel function of KCCA, which can be represented as

$$k(x, y) = e^{-\frac{\|x-y\|^2}{2\sigma^2}} \quad (10)$$

Then the direction of w_x and w_y can be represented as the data onto the direction α and β , which are $w_x = X\alpha$ and $w_y = Y\beta$. Let $M_x = X^T X$ and $M_y = Y^T Y$ be kernel matrices corresponding to the two representation. Then v can be represented as

$$v = \frac{\alpha^T M_x M_y \beta}{\sqrt{\alpha^T M_x^2 \alpha \cdot \beta^T M_y^2 \beta}} \quad (11)$$

To force non-trivial learning on the correlation by dealing with the overfitting and finding irrelevant correlations, a regularization is always applied to KCCA. Correlation coefficient v becomes

$$v = \frac{\alpha^T M_x M_y \beta}{\sqrt{(\alpha^T M_x^2 \alpha + k \alpha^T M_x \alpha)(\beta^T M_y^2 \beta + k \beta^T M_y \beta)}} \quad (12)$$

Then the generalized eigenvalue problem becomes

$$(M_x + kI)^{-1} M_y (M_y + kI)^{-1} M_x \alpha = \lambda^2 \alpha \quad (13)$$

Where λ is the eigenvalue corresponding to the eigenvector w_x . Then the whole equation becomes the standard eigenproblem $Ax = \lambda x$. In our experiments, k is set to 0.01. If $k = 0$, then it becomes the standard KCCA. In our work, regularization is found to be useful.

3 EXPERIMENT

In this section, we demonstrate the dataset used in this work. We also describe the details of our experiment methodology as well as the analysis of experiment results.

3.1 Dataset

To evaluate our proposed scheme, we use FRGCv2.0 database (Phillips et al., 2005). The images within the dataset include pose, expression and illumination changes, which is as illustrated in Figure 1. We randomly choose 300 subjects from FRGCv2.0. For each subject, two visible texture images and two corresponding 3D range images are selected. The whole database is divided into two parts, training set and testing set. The training set contains the 2D-3D pairs of 225 subjects, and the testing set includes other 75 subjects. Note that in all of our experiments, there is no overlap between the training and testing data. This means the images of the same individual are never used in the training and testing phase at the same time.

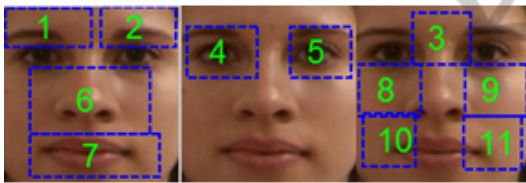


Figure 4: Illustration of face parts division. To be concise, only 2D face image is used. 3D face images also follow the same division scheme.

3.2 Pre-processing

To get the depth image, we follow the procedure in (Xu et al., 2009). The main problem for obtaining the depth image from 3D point cloud is the noise removal and hole filling. To reduce the noise, we apply the mean value filter with the kernel size 5×5 centered with evaluating pixel. If the absolute difference between the central pixel and mean value is greater than our predefined threshold, then this pixel will be regarded as an outlier and replaced. Linear interpolation based on the neighboring pixels is applied to calculate the value of the center pixel value and used to fill the hole.

Before conducting the experiments, all 2D and 3D images are aligned and cropped to the same size, 128×128 pixels, based on eyes coordinates. Since there are many variations (expression, pose), instead of using the whole face (Huang et al., 2010), we use facial parts. The regions of our face parts are illustrated in Figure 4. Different from (Yang et al., 2008),

the parts used in our experiment have semantic meaning, e.g. eyebrow, eyes, nose, mouth, cheeks and etc. Because there are pose and expression changes in FRGCv2.0, we adopt the method for face division in (Kumar et al., 2009). Each extracted face part is enlarged to alleviate the influence brought by these factors. The division of the face is illustrated in Figure 4.

3.3 Learning Scheme and Matching

Pixel intensity is used as the feature in this work. Let us assume the 2D/3D feature pairs in each face part are given as (F_{2d}, F_{3d}) . Then PCA whitening is applied to the feature pairs separately. The output feature pairs are noted as (F'_{2d}, F'_{3d}) . In our work, we set 24 as the dimension of PCA whitening. Feature mean value normalization is also applied. Then GRBM is used to get the representation of (F'_{2d}, F'_{3d}) separately. The hidden layer variables extracted using GRBM model are (F^h_{2d}, F^h_{3d}) . After correlation learning, we can obtain two projection directions W_{2d} and W_{3d} . (F^h_{2d}, F^h_{3d}) are projected into the shared subspace using $x = w_x^T F^h_{2d}$ and $y = w_y^T F^h_{3d}$. w_x and w_y are obtained during the training process. Then the similarity score $s(x, y)$ can be obtained using the following normalized score function:

$$s(x, y) = \frac{x \cdot y}{(\|x\| \cdot \|y\|)} \quad (14)$$

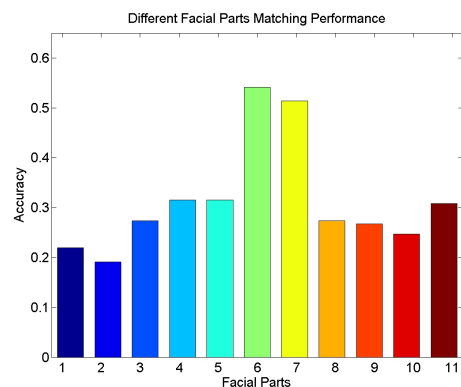


Figure 5: A bar plot of matching accuracy of different facial parts. The number listed here corresponds to the face part number in Fig 4. The results listed here are based on GRBM+rKCCA scheme.

3.4 Experiment Results and Analysis

As described above, we want to investigate the performance of different facial parts for 2D/3D face recognition. As far as we know, this is the first time that the effectiveness of different face parts for 2D-3D face recognition has been evaluated.

Table 1: Assignment of weight for each facial part. The number is the same as illustrated in Fig.4.

Face Part #	1	2	3	4	5	6	7	8	9	10	11
w_t	0.25	0.25	0.25	0.30	0.30	0.50	0.35	0.15	0.15	0.10	0.10

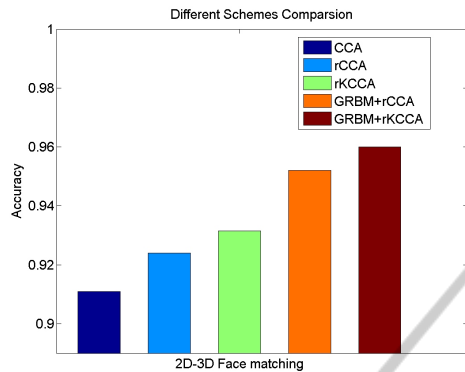


Figure 6: A bar plot of matching accuracy of different algorithms.

Table 2: Performance of different schemes comparison.

Model	Accuracy
CCA	0.911
rCCA	0.924
rKCCA	0.931
GRBM+rCCA	0.952
GRBM+rKCCA	0.960

From our experimental results listed in Figure 5, we find that there is a significant difference among face parts for face recognition. The facial part near the nose region plays the most important role in the matching scheme. Considering the different matching accuracy of each part, the weighed sum rule (Jain et al., 2011) is used as the fusion tool to obtain the final result. Weighted sum rule can be represented as

$$F = \sum_{t=1}^n w_t s_t, \quad (15)$$

where F is the matching score and n is the total number of face parts. w_t is the weight value corresponding to the matching score s_t of face part t . The assignment of value w_t for each facial part is illustrated in Table 1. The matching results after different face parts fusion are shown in Table 2. A better matching result is obtained after fusion of different face parts. From the results listed in Figure 6, we find that RBM can boost the performance of correlation mapping.

In this paper, we also evaluate the proposed algorithm using the global face. The accuracy is 55.0% (based on GRBM+rKCCA). This result also demonstrates that the single global face mapping between 2D and 3D face data is not appropriate for describing the relationship between 2D and 3D face data.

Since the correspondence of different face parts between 2D and 3D is not identical, it's not accurate to use the whole face for correlation learning between two modalities.

4 CONCLUSIONS

In this paper, one single-layer network was proposed for heterogeneous 2D/3D face recognition problem. Our experiment results proved that learning correlation representation on the layer features extracted using RBM resulted in a better matching performance. Meanwhile, we also explored the effectiveness of different facial parts in 2D/3D face matching. The results indicated that fusion with different facial parts can achieve a significant improvement compared with the global face.

The proposed scheme is an excellent addition to the corpus of heterogeneous face recognition works. The proposed learning scheme can also be adopted by other 2D/3D face recognition works as the major learning scheme.

REFERENCES

- Bengio, Y. (2009). Learning deep architectures for ai. *Foundations and trends® in Machine Learning*, 2(1):1–127.
- Dhillon, P., Foster, D. P., and Ungar, L. H. (2011). Multi-view learning of word embeddings via cca. In *Advances in Neural Information Processing Systems*, pages 199–207.
- Guo, G. and Wang, X. (2012). A study on human age estimation under facial expression changes. In *Computer Vision and Pattern Recognition (CVPR), 2012 IEEE Conference on*, pages 2547–2553. IEEE.
- Hardoon, D. R., Szedmak, S., and Shawe-Taylor, J. (2004). Canonical correlation analysis: An overview with application to learning methods. *Neural Computation*, 16(12):2639–2664.
- Hinton, G. E. and Salakhutdinov, R. R. (2006). Reducing the dimensionality of data with neural networks. *Science*, 313(5786):504–507.
- Hotelling, H. (1936). Relations between two sets of variates. *Biometrika*, 28(3/4):321–377.
- Huang, D., Ardabilian, M., Wang, Y., and Chen, L. (2010). Automatic asymmetric 3d-2d face recognition. In *Pattern Recognition (ICPR), 2010 20th International Conference on*, pages 1225–1228. IEEE.

- Huang, D., Ardabilian, M., Wang, Y., and Chen, L. (2012). Oriented gradient maps based automatic asymmetric 3d-2d face recognition. In *Biometrics (ICB), 2012 5th IAPR International Conference on*, pages 125–131. IEEE.
- Jain, A. K., Ross, A. A. A., and Nandakumar, K. (2011). *Introduction to biometrics*. Springer.
- Kim, T.-K., Wong, S.-F., and Cipolla, R. (2007). Tensor canonical correlation analysis for action classification. In *Computer Vision and Pattern Recognition, 2007. CVPR'07. IEEE Conference on*, pages 1–8. IEEE.
- Kumar, N., Berg, A. C., Belhumeur, P. N., and Nayar, S. K. (2009). Attribute and simile classifiers for face verification. In *Computer Vision, 2009 IEEE 12th International Conference on*, pages 365–372. IEEE.
- Li, A., Shan, S., Chen, X., and Gao, W. (2009). Maximizing intra-individual correlations for face recognition across pose differences. In *Computer Vision and Pattern Recognition, 2009. CVPR 2009. IEEE Conference on*, pages 605–611. IEEE.
- Mohamed, A.-r., Dahl, G. E., and Hinton, G. (2012). Acoustic modeling using deep belief networks. *Audio, Speech, and Language Processing, IEEE Transactions on*, 20(1):14–22.
- Ngiam, J., Khosla, A., Kim, M., Nam, J., Lee, H., and Ng, A. (2011). Multimodal deep learning. In *Proceedings of the 28th International Conference on Machine Learning (ICML-11)*, pages 689–696.
- Phillips, P. J., Flynn, P. J., Scruggs, T., Bowyer, K. W., Chang, J., Hoffman, K., Marques, J., Min, J., and Worek, W. (2005). Overview of the face recognition grand challenge. In *Computer vision and pattern recognition, 2005. CVPR 2005. IEEE computer society conference on*, volume 1, pages 947–954. IEEE.
- Rama, A., Tarres, F., Onofrio, D., and Tubaro, S. (2006). Mixed 2d-3d information for pose estimation and face recognition. In *Acoustics, Speech and Signal Processing, 2006. ICASSP 2006 Proceedings. 2006 IEEE International Conference on*, volume 2, pages II–II. IEEE.
- Riccio, D. and Dugelay, J.-L. (2005). Asymmetric 3d/2d processing: a novel approach for face recognition. In *Image Analysis and Processing-ICIAP 2005*, pages 986–993. Springer.
- Sargin, M. E., Yemez, Y., Erzin, E., and Tekalp, A. M. (2007). Audiovisual synchronization and fusion using canonical correlation analysis. *Multimedia, IEEE Transactions on*, 9(7):1396–1403.
- Shotton, J., Fitzgibbon, A., Cook, M., Sharp, T., Finocchio, M., Moore, R., Kipman, A., and Blake, A. (2011). Real-time human pose recognition in parts from single depth images. In *Computer Vision and Pattern Recognition (CVPR), 2011 IEEE Conference on*, pages 1297–1304. IEEE.
- Slaney, M. and Covell, M. (2000). Facesync: A linear operator for measuring synchronization of video facial images and audio tracks. In *NIPS*, pages 814–820.
- Srivastava, N. and Salakhutdinov, R. (2012). Multimodal learning with deep boltzmann machines. In *Advances in Neural Information Processing Systems 25*, pages 2231–2239.
- Sutton, R. S. and Barto, A. G. (1998). *Reinforcement learning: An introduction*, volume 1. Cambridge Univ Press.
- Vinokourov, A., Cristianini, N., and Shawe-taylor, J. S. (2002). Inferring a semantic representation of text via cross-language correlation analysis. In *Advances in neural information processing systems*, pages 1473–1480.
- Wang, H., Klaser, A., Schmid, C., and Liu, C.-L. (2011). Action recognition by dense trajectories. In *Computer Vision and Pattern Recognition (CVPR), 2011 IEEE Conference on*, pages 3169–3176. IEEE.
- Wang, X., Ly, V., Guo, G., and Kambhampettu, C. (2013). A new approach for 2d-3d heterogeneous face recognition. In *Multimedia (ISM), 2013 IEEE International Symposium on*. IEEE.
- Xu, C., Li, S., Tan, T., and Quan, L. (2009). Automatic 3d face recognition from depth and intensity gabor features. *Pattern Recognition*, 42(9):1895–1905.
- Yang, W., Yi, D., Lei, Z., Sang, J., and Li, S. Z. (2008). 2d-3d face matching using cca. In *Automatic Face & Gesture Recognition, 2008. FG'08. 8th IEEE International Conference on*, pages 1–6. IEEE.